Novel Microstrip Multifunction Directional Couplers and Filters for Microwave and Millimeter-Wave Applications

Sener Uysal, *Member, IEEE*, and John Watkins

Abstract—**The design of a new class of microstrip couplers and filters is presented in this paper. The synthesis functions obtained from the solution of first-order nonlinear differential equation of nonuniform lines with a loose coupling assumption are modified and validated for higher coupling values. The design employs a nonuniform coupled line configuration along which a realizable continuous coupling coefficient is obtained by modifying the reflection coefficient distribution function. This modification results in a frequency selective coupling which minimizes the out-of-band coupling in the specified frequency range. As a result it is possible to realize −3 dB directional couplers using double-coupled lines without the need for tandem connections or extreme photolithographic techniques.**

Experimental results for microwave band-pass and periodic couplers are presented together with the computed results. Potential applications of these novel components are discussed and the work is extended to include millimeter-wave realization.

I. Introduction

THE potential applications of nonuniform microstrip directional couplers have not been realized for a number of reasons. Some of these problems can be enumerated as follows: 1) direct synthesis of physical dimensions, 2) isolation, and 3) physical realization. However, solutions to these problems have recently been reported by Uysal *et al.* [1]. This paper continues to investigate other forms and applications of nonuniform microstrip directional couplers.

In directional couplers the coupled arm response is a strong function of frequency. For example, an X-band directional coupler exhibits strong coupling several gigahertz away from its intended bandwidth. Such out-of-band coupling is undesirable and induces practical difficulties in realizing the couplers and limits their application. This paper describes a novel design technique to minimize the out-of-band coupling in nonuniform microstrip directional couplers. Consequently, directional couplers with virtually *any amount of nominal coupling* can be realized without the need for a tandem connection. Furthermore, matched filter performance can be obtained by using the coupled arm response and terminating all other ports. The proposed design technique can readily be extended to include millimeter-wave realization of these components.

Manuscript received September 5, 1990; revised January 30, 1991. This work was supported by the Ministry of Defence, United Kingdom.

The authors are with the Department of Electronic and Electrical Engineering, King's College, London WC2R 2LS, United Kingdom.

IEEE Log Number 9144273.

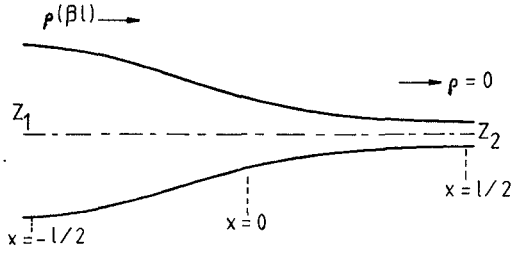

Fig. 1. Nonuniform transmission line section.

Some experimental results have already been reported for a band-pass coupler designed and built on an alumina substrate [2]. Further experimental results for band-pass and periodic couplers will be given in the paper.

II. Design Procedure

An analysis of the nonuniform transmission line shown in Fig. 1 leads to a first-order nonlinear differential equation; the analysis has been given by Klopfenstein [3]. This equation is

$$\frac{d\rho}{dx} - 2\gamma\rho + \frac{1}{2}(1-\rho^2)\frac{d(\ln Z_0)}{dx} = 0 \qquad (1)$$

where ρ is the reflection coefficient at any point along the nonuniform line, γ is the propagation constant, and Z_0 is the characteristic impedance of the line.

Tresselt [4] used a result similar to that given by Sharpe [5] to relate the nonuniform transmission line analysis to the analysis of couplers by postulating that the characteristic impedance curve of the transmission line equals the even-mode impedance curve of the coupler to be analyzed and that the reflection coefficient of the transmission line is equal in magnitude and phase to the coupled-arm response of the coupler.

We now consider two cases of (1); in the first ρ is small and in the second case the relaxation of this restriction is given.

Case 1: $\rho^2 \ll 1$

Under this assumption (1) reduces to

$$\frac{d\rho}{dx} - 2\gamma\rho + p(x) = 0 \qquad (2)$$

0018-9480/91/0600-0977$01.00 ©1991 IEEE

where

$$p(x) = \frac{1}{2}\frac{d}{dx}(\ln Z_{0e}(x)). \tag{3}$$

Equation (2) is a first-order linear differential equation which can be solved for ρ:

$$\rho = -e^{\int_0^x 2\gamma\,dx}\int_0^x e^{-\int_0^x 2\gamma\,dx} p(x)\,dx. \tag{4}$$

Kammler [6] has derived a Fourier transform pair for ρ and $p(x)$:

$$C(\omega) = 2\int_0^{l/2} \sin(2\omega x/v)p(x)\,dx \tag{5}$$

$$p(x) = -\frac{2}{\pi v}\int_0^{2\omega_c} \sin(2\omega x/v)C(\omega)\,d\omega \tag{6}$$

where l is the coupler length with coupler center taken at $x = 0$, v is the velocity in the guide, ω_c is the design center frequency, and $C(\omega)$ is the coupled-arm response, which has replaced ρ of (4). In the above equations γ is replaced by $j\beta = j\omega/v$ by assuming a lossless line.

The above formulation (eqs. (1)–(6)) is valid for a homogeneous medium (TEM propagation) only. For microstrip, in general, the velocity, v, coupling, $C(\omega)$, and the reflection coefficient distribution function, $p(x)$, take subscripts e and o, denoting even and odd modes, respectively. Thence the final solution is obtained by the superposition of the two modes. However, with phase velocity compensation ($v_o = v_e = v$) and double-coupled lines only [1], the above formulation is still valid.

The characteristic impedance, Z_0, can be expressed in terms of even- and odd-mode characteristic impedances of the coupled lines by

$$Z_0^2(x) = Z_{0e}(x)Z_{0o}(x). \tag{7}$$

Normalizing this equation, we have

$$Z_{0e}(x)Z_{0o}(x) = 1. \tag{8}$$

Hence, (3), (5), and (6) are equally valid for the even and odd modes under proper substitution of the corresponding values.

Case 2: Larger Values for ρ

Equations (5) and (6) are no longer valid for larger values of ρ. Tresselt [4] has shown by using Youla's formulation [7] that a second-order coupling leads to

$$|C(\omega)| = \frac{\left|2\int_0^{l/2}\sin\left(\frac{2\omega x}{v}\right)p(x)\,dx\right|}{\sqrt{1+\left|2\int_0^{l/2}\sin\left(\frac{2\omega x}{v}\right)p(x)\,dx\right|^2}}. \tag{9}$$

For larger values of ρ even this result is no longer valid, and Bergquist [8] has reported a series solution for (1) valid at arbitrary load conditions. Under matched conditions, Bergquist's equation (3) becomes, in the context of this paper,

$$|C_{e,o}(\omega)| = \frac{G + G^3/3! + G^5/5! + \cdots}{1 + G^2/2! + G^4/4! + G^6/6!} \tag{10}$$

where

$$G = \left|2\int_0^{l/2}\sin(2\omega x/v_{e,o})p_{e,o}(x)\,dx\right|.$$

Equation (10) can be simplified as

$$|C_{e,o}(\omega)| = \tanh(G). \tag{11}$$

This is an exact closed-form solution of the first-order nonlinear differential equation given by (1), under matched conditions. The direct output is given by

$$|D_{e,o}(\omega)| = \frac{1}{\cosh(G)}. \tag{12}$$

With the above solution for $C_{e,o}(\omega)$, we then have the new transform pair:

$$U_{e,o}(\omega) = 2\int_0^{l/2}\sin(2\omega x/v_{e,o})p_{e,o}(x)\,dx \tag{13}$$

$$p_{e,o}(x) = -\frac{2}{\pi v_{e,o}}\int_0^{2\omega_c}\sin(2\omega x/v_{e,o})U_{e,o}(\omega)\,d\omega \tag{14}$$

where $U_{e,o}(\omega) = \tanh^{-1}(C_{e,o}(\omega))$.

Once $p(x)$ is determined from (14), the continuous coupling coefficient, $k(x)$, of the nonuniform coupler can be determined by first obtaining the characteristic impedances from (3) and then using the following relationship:

$$k(x) = \frac{Z_{0e}(x) - Z_{0o}(x)}{Z_{0e}(x) + Z_{0o}(x)} \tag{15}$$

or

$$k(x) = \frac{e^{2\int_0^x p_e(x)\,dx} - e^{2\int_0^x p_o(x)\,dx}}{e^{2\int_0^x p_e(x)\,dx} + e^{2\int_0^x p_o(x)\,dx}}. \tag{16}$$

This completes the main design procedure for nonuniform directional couplers with any amount of desired coupling. Kammler has derived closed-form relations [6, eqs. (12)–(17)] for an $N_{\Delta x}$ discrete section symmetrical coupler. His equations require a knowledge of $k_d(x)$ discrete coupling coefficients, which are obtained by an optimization process. In our case $k(x)$ is synthesized and readily available through (16). Thus, we can use this $k(x)$ to compare our result, (11), with his formulation [6, eqs. (12)–(17)]. Comparisons are made for a -3 dB and -0.1 dB 11-quarter-wavelength-long couplers in the 0–20 GHz bandwidth. These results are shown in Fig. 2. No attempt has been made to optimize the responses. Our results are slightly lower than Kammler's because of numerical solution of $U_{e,o}(\omega)$ and the fact that the constant of integration is neglected in the solution of the differential equation.

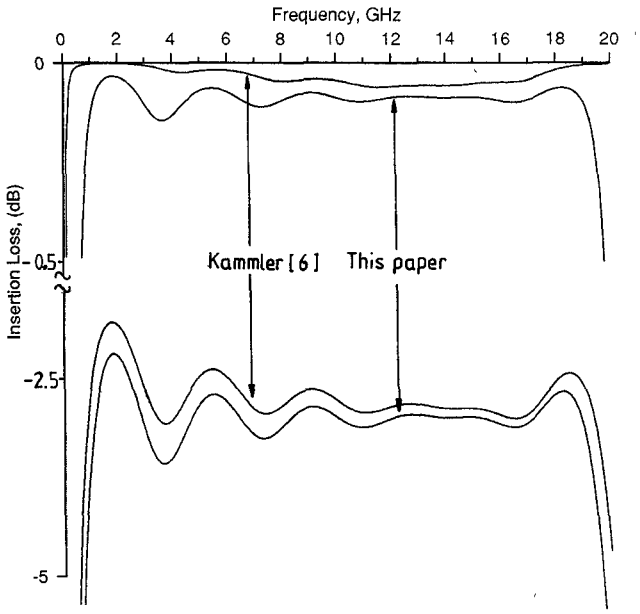

Fig. 2. Comparison of the results of this paper with Kammler's formulation [6, eqs. (12)–(17)] for −3 dB and −0.1 dB couplers.

Band-Pass Couplers

For wide-band tight coupling (of the order of −3.0 dB), the above procedure does not yield a realizable continuous coupling coefficient; instead, a tandem connection of two −8.34 dB couplers is required [1]. However, even for smaller bandwidths the continuous coupling coefficient function is still too high. We shall now illustrate the method of minimizing unwanted coupling in a specified frequency range in order to obtain couplers of the band-pass type.

In order to obtain the reflection coefficient distribution function for the band-pass coupler, $p(x)$ of (14) needs some modifications. It can be shown by using simple integration theorems that if a function is continuous except for a finite number of finite discontinuities in the interval of integration, the function is integrable. Therefore, for a band-pass coupler we can rewrite (14) as follows:

$$p_{e,o}(x) = -\frac{2}{\pi v_{e,o}}\left\{\int_0^{\omega_1} \sin(2\omega x/v_{e,o})U_{e,o}(\omega)_1 d\omega + \int_{\omega_1}^{\omega_2} \sin(2\omega x/v_{e,o})U_{e,o}(\omega)_2 d\omega + \int_{\omega_2}^{2\omega_c} \sin(2\omega x/v_{e,o})U_{e,o}(\omega)_3 d\omega\right\} \quad (17)$$

where e and o denote the even and odd modes, respectively, ω_1 and ω_2 are the lower and upper band edges of the passband, ω_c is the center frequency of the coupler, and $U_{e,o}(\omega)_1, U_{e,o}(\omega)_2$, and $U_{e,o}(\omega)_3$ are the coupling responses in the respective bands. $U_{e,o}(\omega)_1$ and $U_{e,o}(\omega)_3$ can be set to nonzero but very small values [2]. Throughout this paper, out-of-band couplings will be specified as zero. However, the selection of $U_{e,o}(\omega)_2$ depends on the design bandwidth, the center frequency, and the coupler length. Specifying this coupling as a constant value k, for $\omega_1 \leqslant \omega \leqslant \omega_2$, (17) can be solved as

$$p_{e,o}(x) = \frac{2k}{\pi x}\sin[(\omega_2+\omega_1)x/v_{e,o}] \cdot \sin[(\omega_2-\omega_1)x/v_{e,o}]. \quad (18)$$

It can be shown that one of the problems in the design procedure is the selection of phase velocity, $v_{e,o}$. Normally, this value is selected to correspond to that of the design center frequency. However, for long coupler lengths and wide-band multifunction operation, the overall performance deteriorates (higher out-of-band coupling) owing to the variation in the phase velocity. In general, the phase velocity is a three-dimensional function: $v_{e,o}(x,\omega)$. Therefore, $x/v_{e,o}$ in (13) should be replaced by $\int_0^x dx/v_{e,o}(x,\omega)$. Assuming a linear variation in phase velocity with respect to x, it can be deduced that

$$\int_0^x \frac{dx}{v_{e,o}(x,\omega)} = \frac{l}{2\left(v_{e,o_2}(\omega)-v_{e,o_1}(\omega)\right)} \cdot \ln\left[1+2\frac{\left(v_{e,o_2}(\omega)-v_{e,o_1}(\omega)\right)}{l v_{e,o_1}(\omega)}x\right] \quad (19)$$

where $v_{e,o_1}(\omega)$ and $v_{e,o_2}(\omega)$ are the phase velocities at $x=-l/2$ and $x=0$, respectively.

Although the phase velocities are compensated, i.e, even-mode phase velocities are equal to the odd-mode phase velocities, the design is kept general in the sense that an interdigitated section (nonuniform Lange [1]) may be required in some cases. However, the length of the interdigitated section need not be a full $\lambda/4$ [2].

The computational procedure is iterative starting with the computation of a reflection coefficient distribution function with specified coupling value in the desired passband. The coupling function is then computed and the procedure is repeated until an optimum realizable continuous coupling coefficient is achieved.

In order to have a realizable continuous coupling coefficient, the following relationship must be satisfied:

$$Z_{0e}(x) \geqslant 1.0 \qquad \forall x \quad (20)$$

where $Z_{0e}(x)$ is the normalized even-mode characteristic impedance of the coupler. For the band-pass coupler, since we define $\omega_1 > 0.0$, the outcome of (16) obtained by using (17) and a specified nominal coupling in the passband is not a realizable function (i.e., *some* $k(x) < 0.0$). This can be corrected by defining a new reflection coefficient distribution function. However, the relationship between $p(x)$ and $k(x)$ is nonlinear. Therefore, a number of generalized methods will now be investigated to find a realizable $k(x)$ by modifying the computed $p(x)$.

Method 1

A new reflection coefficient distribution function will be defined by adding a constant to the computed $p(x)$:

$$p_{e,o_A}(x) = p_{e,o}(x) + A_{e,o} \quad (21)$$

where $p_{e,o}(x)$ is given by (16), and $A_{e,o}$, which is to be determined, satisfies the following relationship:

$$A_{e,o} = \begin{cases} \pm A, & -\frac{l}{2} \leqslant x \leqslant 0 \\ \mp A, & 0 \leqslant x \leqslant \frac{l}{2} \\ 0, & \text{otherwise.} \end{cases} \tag{22}$$

The corresponding coupling function, $U_{e,o_A}(\omega)$, is obtained by

$$U_{e,o_A}(\omega) = F\{p_{e,o}(x) + A_{e,o}\} = F\{p_{e,o}(x)\} + F\{A_{e,o}\} \tag{23}$$

where F denotes Fourier transform. Hence

$$U_{e,o_A}(\omega) = U_{e,o}(\omega) - j\frac{A_{e,o}v_{e,o}}{\omega}\sin^2\left(\frac{\omega l}{2v_{e,o}}\right). \tag{24}$$

The constant A can be determined by using (3) as follows:

$$Z_{0e_A}(x) = e^{2\int_0^x p_e x + A\,dx}. \tag{25}$$

For a realizable $Z_{0e_A}(x)$, we have

$$e^{2\int_0^x p_e(x) + A\,dx} \geqslant 1.0 \tag{26}$$

or

$$A \geqslant \frac{1}{2l}\ln\left(\frac{1}{Z_{0e}(x)_{\min}}\right) \tag{27}$$

where $Z_{0e}(x)_{\min}$ is the minimum value obtained with $A = 0$.

Method 2

The second method is to add a linear function to computed, $p(x)$:

$$p_{e,o_B}(x) = p_{e,o}(x) + B_{e,o} \tag{28}$$

where $B_{e,o}$ is given by

$$B_{e,o} = \begin{cases} \mp\frac{2B_x}{l}, & |x| \leqslant \frac{l}{2} \\ 0, & |x| > \frac{l}{2}. \end{cases} \tag{29}$$

The corresponding coupling function, $U_{e,o_B}(\omega)$, is obtained by

$$U_{e,o_B}(\omega) = U_{e,o} \mp j\frac{Bv_{e,o}}{\omega}\left\{\cos\left(\frac{\omega l}{v_{e,o}}\right) - \frac{v_{e,o}}{\omega l}\sin\left(\frac{\omega l}{v_{e,o}}\right)\right\}. \tag{30}$$

The constant B is given by

$$B \geqslant \frac{1}{2l}\ln\left(\frac{1}{Z_{0e}(x)_{\min}}\right) \tag{31}$$

where $Z_{0e}(x)_{\min}$ is the minimum value obtained with $B = 0$.

Method 3

The computed even-mode impedance will be multiplied by a constant such that the resultant normalized even-mode impedance is greater or equal to 1.0:

$$Z_{0e,o_E}(x) = Z_{0e,o}(x)e^{E_{e,o}} \tag{32}$$

where $e^{E_{e,o}}$ is given by

$$e^{E_{e,o}} = e^{\pm E}. \tag{33}$$

The new reflection coefficient distribution function in this case is given by

$$p_{e,o_E}(x) = \frac{1}{2}\frac{d}{dx}\ln Z_{0e,o}(x) \pm \frac{1}{2}\frac{d}{dx}E_{e,o} \tag{34}$$

or

$$p_{e,o_E}(x) = p_{e,o}(x) \pm \left\{\frac{1}{2}E\delta\left(x + \frac{l}{2}\right) - \frac{1}{2}E\delta\left(x - \frac{l}{2}\right)\right\}. \tag{35}$$

The corresponding coupling function is given by

$$U_{e,o_E}(\omega) = U_{e,o}(\omega) \pm \frac{E}{2}\{e^{j\omega l/v_{e,o}} - e^{-j\omega l/v_{e,o}}\}$$

$$= U_{e,o}(\omega) \pm jE\sin\left(\frac{\omega l}{v_{e,o}}\right) \tag{36}$$

and the constant E is given by

$$E \geqslant \ln\left(\frac{1}{Z_{o,e}(x)_{\min}}\right) \tag{37}$$

where $Z_{o,e}(x)_{\min}$ is the minimum value obtained with $E = 0$.

In the equations of the presented methods, alternate signs are used to avoid duplicated equations, the top sign being for the even-mode.

Comparison of Methods

The methods presented above all produce realizable continuous coupling coefficient functions. This will be illustrated by an example: A -3 dB band-pass coupler with $f_1 = 11$ GHz and $f_2 = 15$ GHz, frequency range = 0–20 GHz, and a length of eight quarter wavelengths is considered. The computed results for $k(x)$ (without modification), together with $k_A(x)$, $k_B(x)$, and $k_E(x)$ for, respectively, the three methods presented, and their respective performances (not optimized), are shown in Fig. 3.

In the first two methods $k_A(x)$ and $k_B(x)$ start from a minimum value ($k_A(-l/2) = k_B(-l/2) \approx 0.0$). In the third method, $k_E(x)$ is shifted up as a result of multiplying $Z_{0o,e}(x)$ by a constant value. $k_A(x)$ produced by the first method gives higher coupling coefficients at the center. This is an expected result since we add/subtract the same constant value to/from $p_{e,o}(x)$. $k_B(x)$ of the second method is somewhat scaled since $p_{e,o}(x)$ is modified by a linear function. In the third method, $k_E(-l/2)$ is always greater than 0.

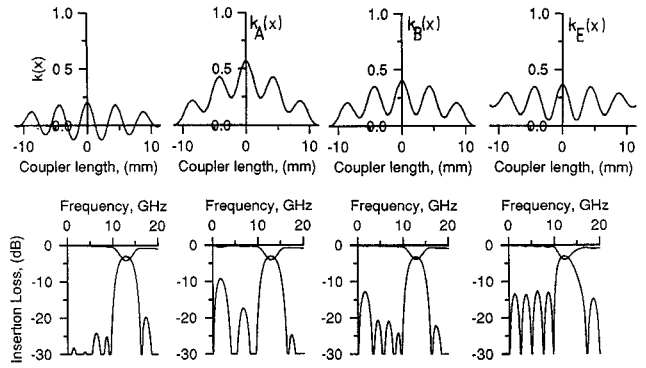

Fig. 3. Unrealizable continuous coupling coefficient $k(x)$ and modified continuous coupling coefficients $k_A(x)$, $k_B(x)$, and $k_E(x)$ for the three methods, respectively, and their respective performances (not optimized) for a -3 dB band-pass coupler with $f_1 = 11$ GHz, $f_2 = 15$ GHz, and $l = 8\ \lambda_c/4$.

All three methods can be used depending on the application, bandwidth, coupler length, and center frequency of the design. Since the factors affecting the choice of method are many, for the time being, optimization of the respective performance is carried out by generating an error function for the coupling response in the passband and slightly changing the length and/or increasing the value of constants (A, B, E) depending on the taper rate and/or maximum and/or minimum coupling coefficients.

Periodic Couplers

The design procedure can be further modified to design periodic couplers. For this case the reflection coefficient distribution function is given by

$$P_{e,o}(x) = -\frac{2}{\pi v_{e,o}}\left\{\int_0^{\omega_1} \sin(2\omega x / v_{e,o}) U_{e,o}(\omega)_1\, d\omega + \int_{\omega_1}^{\omega_2} \sin(2\omega x / v_{e,o}) U_{e,o}(\omega)_2\, d\omega + \int_{\omega_2}^{\omega_3} \sin(2\omega x / v_{e,o}) U_{e,o}(\omega)_3\, d\omega + \int_{\omega_3}^{\omega_4} \sin(2\omega x / v_{e,o}) U_{e,o}(\omega)_4\, d\omega\right\} \quad (38)$$

where e and o denote the even and odd modes, respectively, $v_{e,o}$ is the velocity in the guide, and $U_{e,o}(\omega)_i$ $(i = 1,2,3,4)$ is the specified coupling for each channel.

For low gigahertz frequencies the coupling requirements are more stringent; therefore in the first channel $U_{e,o}(\omega)$ will be set to be equal to zero, allowing the first channel from the direct output. The computed coupling coefficient with $f_1 = 6.0$ GHz, $f_2 = 10.0$ GHz, $f_3 = 14.0$ GHz, and $f_4 = 18.0$ GHz is shown in Fig. 4. The corresponding physical parameters are given in Fig. 5. The taper rate is sharper near the center, which might lead to errors in the performance.

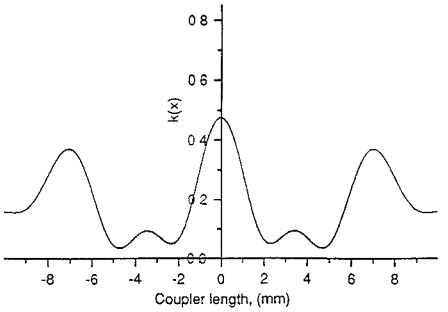

Fig. 4. The computed coupling coefficient function for the periodic coupler with $f_1 = 6.0$ GHz, $f_2 = 10.0$ GHz, $f_3 = 14.0$ GHz, $f_4 = 18.0$ GHz, and $l = 19.8$ mm.

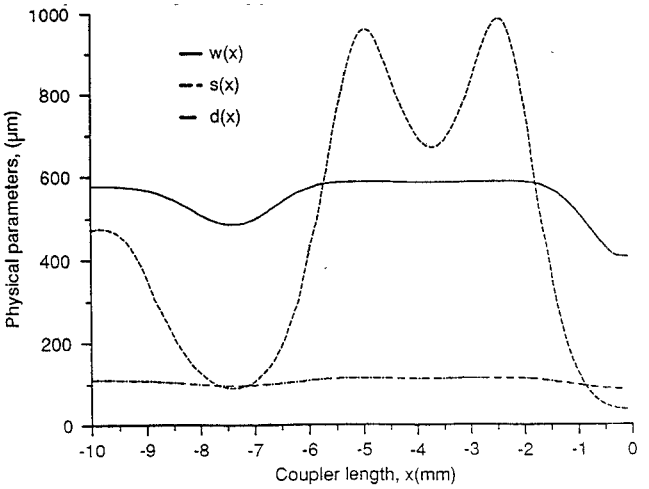

Fig. 5. The computed physical parameters $w(x)$, $s(x)$, and $d(x)$ (at elemental lengths of 0.1 mm) for the periodic coupler with $f_1 = 6.0$ GHz, $f_2 = 10.0$ GHz, $f_3 = 14.0$ GHz, $f_4 = 18.0$ GHz and $l = 19.8$ mm.

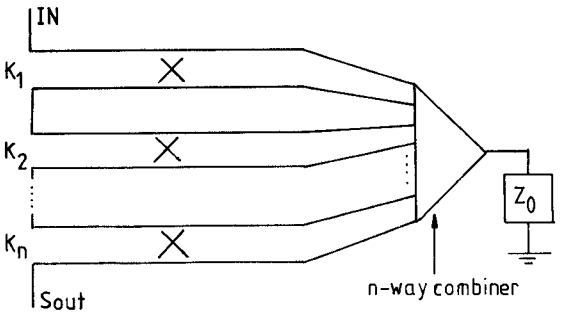

Fig. 6. Proposed band-pass filter using n cascaded couplers.

Filters

One possible way of realizing filters with this design procedure is illustrated in Fig. 6. Several couplers (K_i, $i = 1,2,\cdots,n$) may be cascaded as shown. The unused ports can be terminated in a number of ways; the use of an n-way combiner is suggested for a large number of ports.

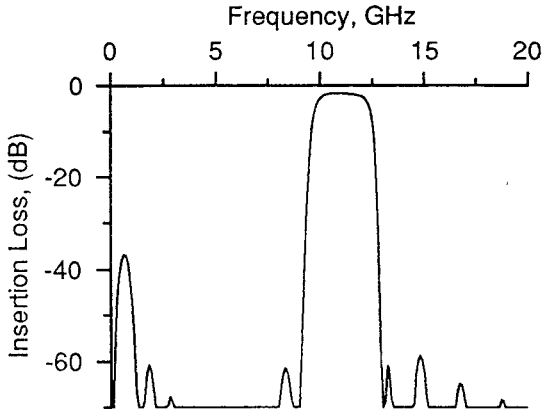

Fig. 7. Computed filter performance with $n = 3$.

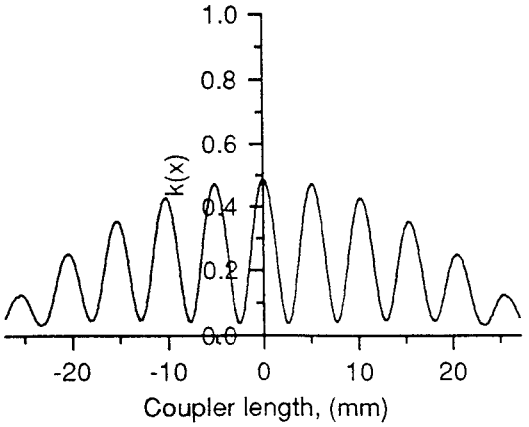

Fig. 8. Computed continuous coupling coefficient for each of the couplers for the band-pass filter.

Assuming identical cascaded sections, the output signal is given by

$$S_{\text{out}} = 20n \log\left\{\frac{C(\omega)}{1+\alpha_T(f)}\right\} \tag{39}$$

where n is the number of cascaded couplers, $C(\omega)$ is the coupled response, and $\alpha_T(f)$ is the frequency-dependent total loss for each coupler. Similar equations can be obtained for the band-pass insertion loss and the stopband attenuation of the filter: $C(\omega)$ is replaced by $C_B(\omega)$ (nominal coupling in the passband) and $C_R(\omega)$ (out-of-band) coupling, respectively.

Example

Band-pass filter specifications:

center frequency, $f_0 = 11$ GHz;
3 dB bandwidth, $B_{3\text{ dB}} = 2$ GHz;
stopband attenuation, $C_R \leqslant -50$ dB;
insertion loss, $S_{\text{out }B} \geqslant -3$ dB;
frequency range = 5–17 GHz;
passband ripple = ± 0.25 dB;
return loss, $RL \leqslant -15$ dB.

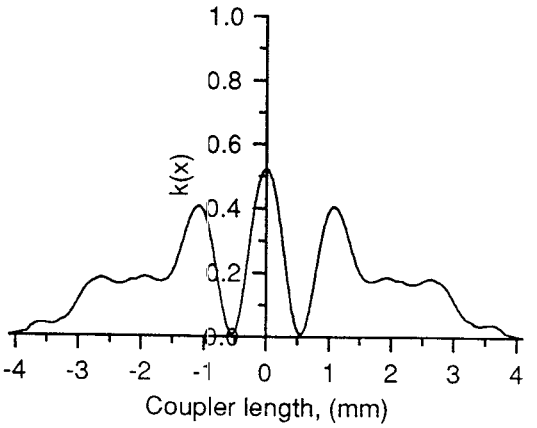

Fig. 9. The computed coupling coefficient for the millimeter-wave coupler with $f_1 = 28.0$ GHz, $f_2 = 48.0$ GHz, and $l = 8.2$ mm.

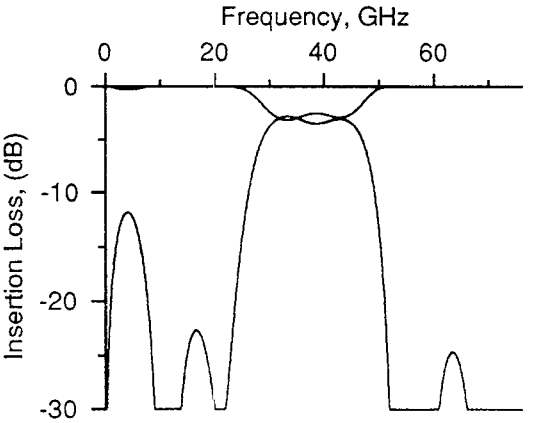

Fig. 10. The computed performance for the millimeter-wave coupler with $f_1 = 28.0$ GHz, $f_2 = 48.0$ GHz, and $l = 8.2$ mm.

The coupled arm response is first computed with $n = 1$ to determine $C_R(\omega)$ for each coupler. Since the size of the filter is not specified, the minimum coupler length which would satisfy the given specifications will be used. The following results are obtained:

number of cascaded couplers, $n = 3$;
nominal band-pass coupling, $C_B(\omega) = 0.99$;
size: length = 54.1 mm, width = 16 mm on 0.625 mm alumina substrate with $\epsilon_r = 9.9$.

The overall coupled response, $S_{\text{out }B}$, is shown in Fig. 7, and the continuous coupling coefficient computed for each of the identical couplers used in this filter is given in Fig. 8.

Millimeter-Wave Band-Pass Couplers

Millimeter-wave directional couplers and filters have applications in satellite communications (e.g. on-board processing, filtering), military communications, measurements, and low-power signal processing techniques. For the synthesis of millimeter-wave nonuniform directional

TABLE I
BAND-PASS COUPLERS

Bandwidth (GHz)	Passband (GHz)	Coupling (dB)	Length (mm)	Max w (mm)	Max s (mm)	Min w (mm)	Min s (mm)
0–20	8–12	−3.0	19.8	0.577	0.490	0.425	0.048
0–20	10–14	−3.0	19.8	0.555	0.470	0.438	0.066
0–20	10–14	−1.2	19.8	0.583	0.987	0.408	0.038

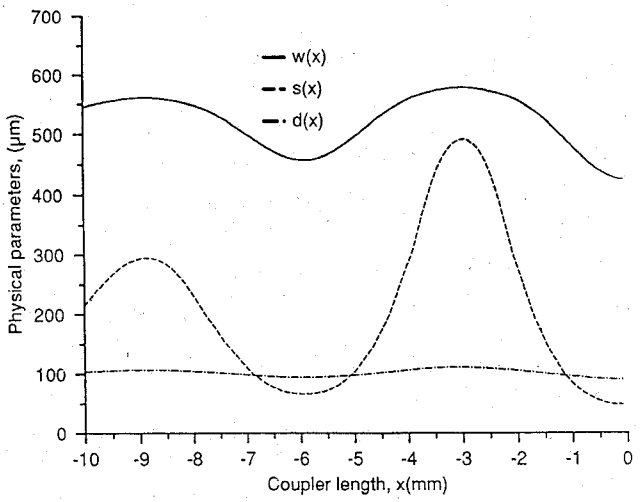

Fig. 11. The computed physical parameters $w(x)$, $s(x)$, and $d(x)$ (at elemental lengths of 0.1 mm) for the band-pass coupler with $f_1 = 8.0$ GHz, $f_2 = 12.0$ GHz, and $l = 19.8$ mm.

couplers a similar design procedure may be followed. The static approximation technique presented in [1] is still applicable with proper compensation for dispersion. Kirschning and Jansen [9] and Hammerstad and Jensen [10] have reported very accurate results with a wide range of applicability. Their results can easily be incorporated with the design technique given in [1]. The following specifications can be used to determine the performance of a millimetric coupler with midband frequency set to be equal to 38 GHz:

impedance level, $Z_0 = 50\ \Omega$;
substrate: alumina, dielectric constant, $\epsilon_r = 9.9$, thickness, $h = 0.25$ mm;
compensated phase velocity, $v_{e,o_1}(\omega) = v_{e,o_2}(\omega) = 110.10^9$ mm/s;
coupler design bandwidth: lower band edge, $f_1 = 28$ GHz, upper band edge, $f_2 = 48$ GHz.

Initially the coupler length was chosen to be 15 quarter wavelengths at 38 GHz. However, the small values of wiggle depths allow us to further reduce the physical length by increasing wiggle depths. Theoretically, maximum wiggle depth should approximately be less than half of the strip width. This reduction in length can be done by using [1, eq. (11)]. Multiplying wiggle depths by a factor of 4, we then obtain the compensated length as 0.546 mm at 38 GHz. This corresponds to a length reduction of 24.5%, giving a total length of 8.2 mm. The computed continuous coupling coefficient, $k(x)$, and the corresponding performance for this design are shown in Figs. 9 and 10, respectively. The losses were not included in the computations.

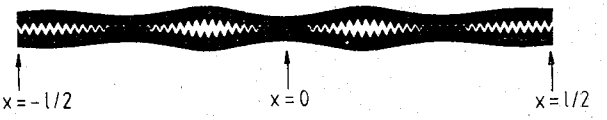

Fig. 12. The positive film (mask) for the band-pass coupler with $f_1 = 8.0$ GHz, $f_2 = 12.0$ GHz, and $l = 19.8$ mm.

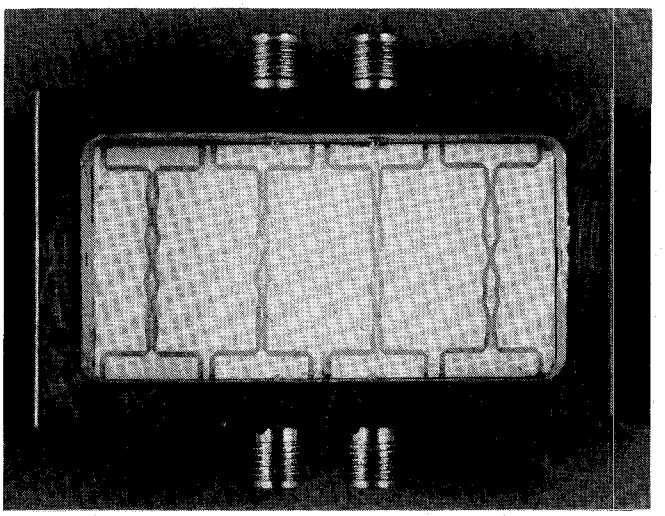

Fig. 13. Photograph of the band-pass and periodic couplers designed and built on alumina substrate.

III. EXPERIMENTAL BAND-PASS COUPLERS

Several band-pass couplers are designed and built on a single alumina substrate. The computational specifications are summarized in Table I.

The continuous physical parameters for these couplers are obtained by the procedure given in [1]. For the first band-pass coupler these are shown in Fig. 11. These computed results show that the variation of parameters along the coupler length is smooth, which ensures minimum error from tapering. The positive film (mask) produced for this design is shown in Fig. 12.

Measured Results

Measurements are carried out on an HP8510B network analyzer. A photograph of the band-pass couplers and the periodic coupler is shown in Fig. 13. The measured results for the first band-pass coupler given in Table I are shown in Fig. 14 (parts (a)–(d)). The measured coupled and

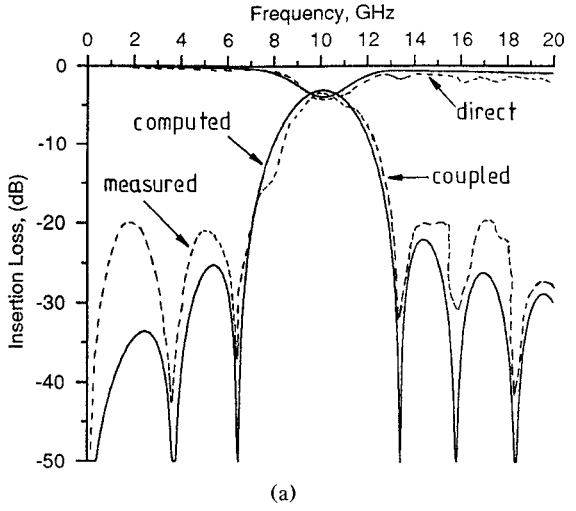

(a)

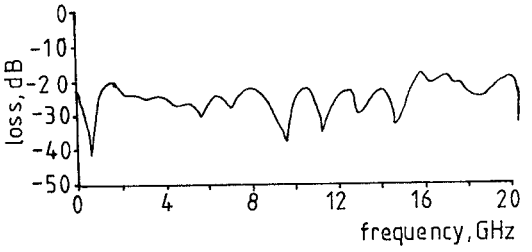

(b)

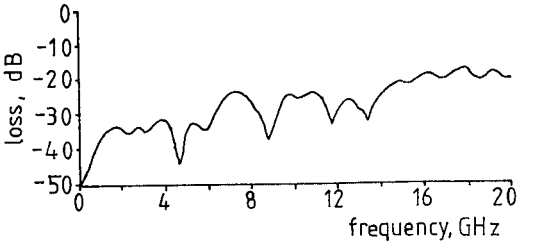

(c)

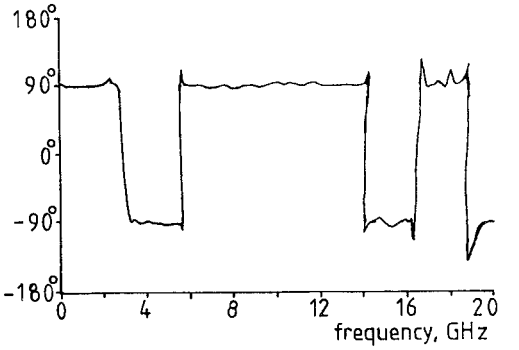

(d)

Fig. 14. The measured performance of the band-pass coupler with $f_1 = 8.0$ GHz, $f_2 = 12.0$ GHz, and $l = 19.8$ mm: (a) comparison of measured coupled and direct ports with computed results (losses are included with the computed results); (b) measured return loss; (c) measured isolation; and (d) measured phase difference between the coupled and direct ports.

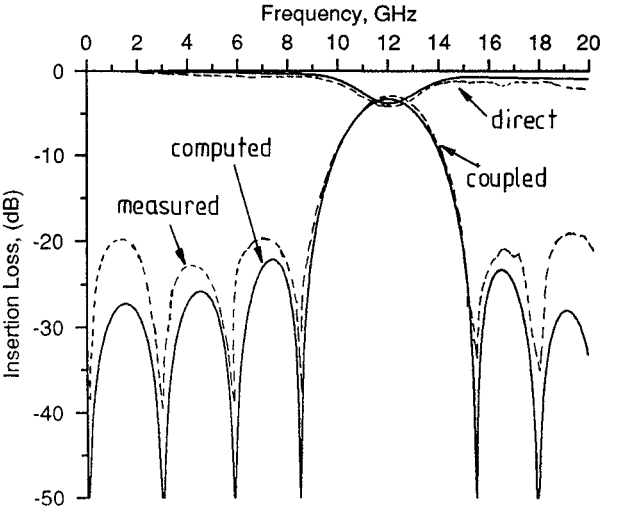

Fig. 15. Comparison of computed and measured coupled and direct ports for the band-pass coupler with $f_1 = 10.0$ GHz, $f_2 = 14.0$ GHz, and $l = 19.8$ mm.

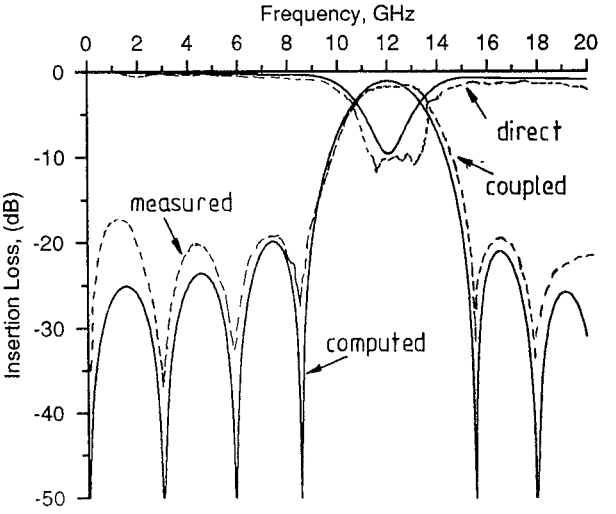

Fig. 16. Comparison of computed and measured coupled and direct ports for the band-pass coupler with $f_1 = 10.0$ GHz, $f_2 = 14.0$ GHz, $l = 19.8$ mm, and a nominal band-pass coupling of -1.2 dB.

direct ports are given in Fig. 14(a) and compared with the computed results. The out-of-band coupling is measured to be -17 dB maximum. Very small ripples were observed in the measured results because the circuits were built close to each other on $25.4 \times 50.8 \times 0.635$ mm^3 alumina substrate. The measured return loss is better than -16 dB in the entire band, and isolation is -22 dB in the 0–14 GHz band. The phase quadrature is good and changes sign at the value of nulls (the change of sign in phase has no physical meaning and is an anomaly of the network analyzer). The results for the second band-pass coupler are shown in Fig. 15. Again, close agreement is observed between the measured and theoretical results. The third band-pass coupler was designed with a nominal coupling of -1.2 dB in the passband and the results are given in Fig. 16.

The measured results for the periodic coupler are shown in Fig. 17; the agreement is good except at the second

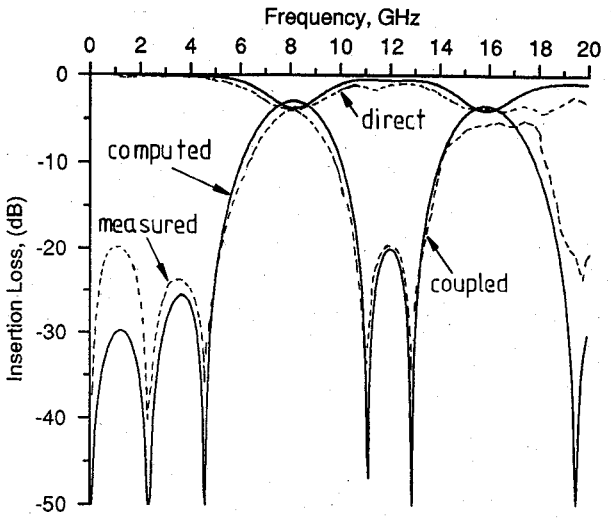

Fig. 17. Comparison of computed and measured coupled and direct ports for the periodic coupler with $f_1 = 6.0$ GHz, $f_2 = 10.0$ GHz, $f_3 = 14.0$ GHz, $f_4 = 18.0$ GHz, and $l = 19.8$ mm (losses are included with the computed results).

passband, where the measured coupling is -1.1 dB less than the predicted value.

IV. Conclusions

A novel design technique has been presented for band-pass and periodic couplers. The design uses a nonuniform wiggly line configuration along which a realizable coupling coefficient is obtained by modifying the reflection coefficient distribution function. This modification results in a frequency selective coupling which minimizes the out-of-band coupling in the specified frequency range.

Good agreement is observed between the theoretical and experimental results. It has also been shown theoretically that the design procedure can be extended for millimeter-wave realizations of these components with proper compensation for dispersion.

Acknowledgment

The authors would like to thank to Ministry of Defence (U.K.) for permission to publish this paper.

References

[1] S. Uysal and A. H. Aghvami, "Synthesis, design and construction of ultra-wide-band nonuniform quadrature directional couplers in inhomogeneous media," *IEEE Trans. Microwave Theory Tech.*, vol. 37, pp. 969–976, June 1989.

[2] J. Watkins and S. Uysal, "Novel microstrip directional band-pass/band-stop couplers and filters," in *1990 IEEE MTT-S Int. Microwave Symp. Dig.*, (Dallas), May 1990, vol. 1, pp. 411–414.

[3] R. W. Klopfenstein, "A transmission line taper of improved design," *Proc. IRE*, vol. 44, pp. 31–35, Jan. 1956.

[4] C. P. Tresselt, "The design and construction of broadband, high-directivity, 90-degree couplers using nonuniform line techniques," *IEEE Trans. Microwave Theory Tech.*, vol. MTT-14, pp. 647–656, Dec. 1966.

[5] C. B. Sharpe, "An alternative derivation of Orlov's synthesis formula for nonuniform lines," *Proc. Inst. Elec. Eng.*, vol. 109, (monograph 483E), pp. 226–229, 1962.

[6] D. W. Kammler, "The design of discrete N-section and continuously tapered symmetrical microwave TEM directional couplers," *IEEE Trans. Microwave Theory Tech.*, vol. MTT-17, pp. 577–590, Aug. 1969.

[7] D. C. Youla, "Analysis and synthesis of arbitrarily terminated lossless nonuniform lines," *IEEE Trans. Circuit Theory*, vol. CT-11, pp. 363–372, Sept. 1964.

[8] A. Bergquist, "Wave propagation on nonuniform transmission lines," *IEEE Trans. Microwave Theory Tech.*, vol. MTT-20, pp. 557–558, Aug. 1972.

[9] M. Kirschning and R. H. Jansen, "Accurate wide-range design equations for the frequency-dependent characteristic of parallel coupled microstriplines," *IEEE Trans. Microwave Theory Tech.*, vol. MTT-32, pp. 83–90, Jan. 1984.

[10] E. Hammerstad and Ø. Jensen, "Accurate models for microstrip computer-aided design," in *1980 IEEE MTT-S Int. Microwave Symp. Dig.*, 1980, pp. 407–409.

Sener Uysal (S'88–M'89) was born in Yigitler, Cyprus, on August 25, 1959. He received the B.Eng. degree (high honours) in electrical engineering from Eastern Mediterranean University, Famagusta, Cyprus, in 1984 and the M.Sc. degree in digital electronics and the Ph.D. degree in electrical engineering from King's College London, University of London, London, England, in 1985 and 1990, respectively. His Ph.D. research resulted in a demonstration of the first microstrip -3 dB, 2–20 GHz quadrature coupler.

Since August 1989 he has been a postdoctoral research fellow at King's College working on projects sponsored by the Ministry of Defence (U.K.) involving microwave and millimeter-wave techniques. His current research interests include couplers, filters, mixers, tunable phase-shifters, microstrip antennas and arrays, and radar. He is also interested in hybrid transferred electron amplifier-mixers (TEAM).

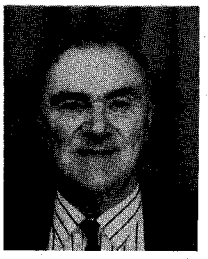

John Watkins graduated with a theoretical physics degree from King's College London in 1948 and spent a number of years in the electronics industry specializing in materials used at microwave frequencies and the measurement techniques associated with their evaluations. He rejoined King's College in 1968 and has worked and published in a number of electronic fields, mostly on microwave topics. His current research includes modeling studies of electromagnetic fields and microwave components using computational procedures.

Mr. Watkins is a Senior Lecturer at King's College and is a Fellow of the IEE (U.K.) and of the Institute of Physics (U.K.).